

IPNO-DRE 98-04

Analyzing powers of one and two Δ production in inelastic p p reactions at energies between 1.5 and 2.1 GeV pp Scattering

J.Yonnet¹, B.Tatischeff², N.Willis², M.Boivin¹,
M.P.Comets², P.Courtat², R.Gacougnolle²,
Y.Le Bornec², E.Loireleux² and F.Reide²

¹ *Laboratoire National Saturne CEA-DSM CNRS-IN2P3
F-91191 Gif-sur-Yvette Cedex, France*

² *Institut de Physique Nucleaire Orsay
F-91406 Orsay Cedex, France*

SW9820



Submitted to Nuclear Physics A

Analyzing powers of one and two Δ production in inelastic $p\bar{p}$ reactions at energies between 1.5 and 2.1 GeV

J. Yonnet^{a1}, B. Tatischeff^b, M.P. Rekalov^{b2}, N. Willis^b,
M. Boivin^a, M.P. Comets^b, P. Courtat^b, R. Gacougnolle^b,
Y. Le Bornec^b, E. Loireleux^b, F. Reide^b

^aLaboratoire National Saturne, CNRS/IN2P3, F-91191 Gif-sur-Yvette Cedex, France

^bInstitut de Physique Nucléaire, CNRS/IN2P3, F-91406 Orsay Cedex, France

Abstract

The reaction $\bar{p}p \rightarrow p\pi^+X$ was studied at three energies ($T_p=1520, 1805$ and 2100 MeV). The analyzing powers of $\bar{p}p \rightarrow \Delta\Delta$, $\bar{p}p \rightarrow \Delta n$ and $\bar{p}p \rightarrow p\pi^+X$ reactions ($.94 < M_X < 1.5$ GeV) were extracted between 0^0 and 17^0 in the lab., which corresponds to an angular range between 0^0 and 100^0 (c.m.). A theoretical analysis was performed based on s-channel contributions in 2^+ and 1^- intermediate states. The resulting formulas allow us to obtain good fits with experimental data.

PACS : 13.75.Cs

Key words: NUCLEAR REACTIONS, polarized protons, analyzing powers in inelastic pp scattering.

1 Introduction

The understanding of nucleon-nucleon (NN) scattering is obviously an important task which deserves a great amount of study. This is a fundamental reaction and moreover its understanding is necessary for the study of other problems in nuclear physics, particularly within conventional meson-baryon

¹ Present address : Institut de Physique Nucléaire, CNRS/IN2P3, F-91406 Orsay Cedex, France.

² Permanent address : National Science Center KFTI 310108 Kharkov, Ukraine.

models.

The NN elastic scattering reactions were extensively studied. Results from these reactions are necessary to obtain phase shift values, to determine the amplitudes and to associate some partial waves to experimentally observed baryonic resonances. The summarizing article [1] presents the results published before 1993 corresponding to the energy range of 100 MeV up to a few GeV (references inside). Since that time, new experimental data concerning p p elastic scattering have been published. They were measured in Indiana [2] (close to 200 MeV) in the coulomb-nuclear interference region, at KEK [3] (in the energy range 0.5 up to 2.0 GeV) and at LAMPF with the study of p p spin correlation functions [4]. After the KEK measurements, new Phase Shift Analyses were proposed for pp elastic scattering between 0.5 and 1 GeV [5]. There has also been new data concerning n p elastic scattering measured at Saturne [6] and LAMPF [7].

However at intermediate energies, the elastic channel is largely coupled to inelastic channels, and these have been less extensively studied. At the energies studied here, multi pion production can be neglected and only four reactions should be considered, namely the production of πd , πNN , ΔN and $\Delta\Delta$. The πd channel, which is experimentally the easiest to study, received most of the attention. Using polarized proton beams, spin observables from that reaction have supplied important constraints and therefore have been useful to improve our knowledge on N-N interaction. The main experimental results obtained up to 1989 in inelastic N-N scattering experiments, were reported and discussed in [8] (references inside). Since 1989, new different experiments concerning inelastic NN scattering, were performed at LAMPF, at 800 MeV and below, and at KEK where $n p \rightarrow p p \pi^-$ reaction was studied [9] between 1.0 and 1.9 GeV/c. At LAMPF different experiments were performed. The corresponding publications deal with the study of spin dependence of pp inelasticities, $\bar{p} p \rightarrow p \pi^+ n$ reaction [10], $\bar{p} p \rightarrow d \pi^+$ [11] and spin correlation parameters for $p p \rightarrow d \pi^+$ [12]. Some properties of the N-N interaction were emphasized by more sophisticated experiments such as those combining inelastic scattering with spin observables. As an example let us recall the asymmetry $\Delta\sigma_L(\bar{p}\bar{p} \rightarrow NN\pi)$ as a function of incident beam momentum, measured at LAMPF. The data [13] was compared to different calculations, namely the Deck model calculations, or those performed by Kloet et al. and Rinat et al. (see ref.[13]). The agreement with experimental results could only be obtained with an admixture of dibaryons.

A combined analysis of $p p \rightarrow p p$, $\pi d \rightarrow \pi d$ and $\pi d \rightarrow pp$ reactions was performed recently in the energy range from pion production threshold up to $\sqrt{s} = 2.44$ GeV [14].

A progress report describing the various theoretical approaches concerning the πNN system (NN or $\pi d \rightarrow NN$, πd or πNN) was published some years ago [15] [8] (references inside). The authors concluded that they needed additional inelastic scattering data in order to constrain the coupled-channel analysis. New theoretical papers have been published recently [16]. Some of them analyze

the link between six-quark configuration and baryon-baryon scattering [17] as being connected to the possible existence of broad dibaryons. The tensor polarization T_{20} in elastic πd scattering was investigated [18] and the importance of the Pauli exchange contribution was confirmed. The effect of two-term potentials in the P_{33} and P_{11} πN channels for the πNN system was studied [19]. The $NN \rightarrow \Delta N$ transition amplitude analysis has been recently performed within the density matrix formalism [20].

2 Experiment

In this paper we will present data on NN inelastic channels, namely the analyzing powers of $\bar{p} p \rightarrow \Delta \Delta$, Δn and $p \pi^+ n$ reactions (for $p \pi^+$ invariant masses larger than 1300 MeV) at three incident proton energies : 1520, 1805 and 2100 MeV. The measurements were carried out using the polarized proton beam from Saturne synchrotron and the SPES3 facility [21]. The spectrometer was set at several different angles between 0° and 17° (lab.) and the data of all the angles (at the same energy) was mixed in order to obtain data (in c.m.) between 0° and θ_{max} ($\theta_{max}=100^\circ$ for $\bar{p} p \rightarrow \Delta \Delta$, at 1805 MeV). Both particles, p and π^+ were detected in coincidence in the solid angle of 10^{-2} sr

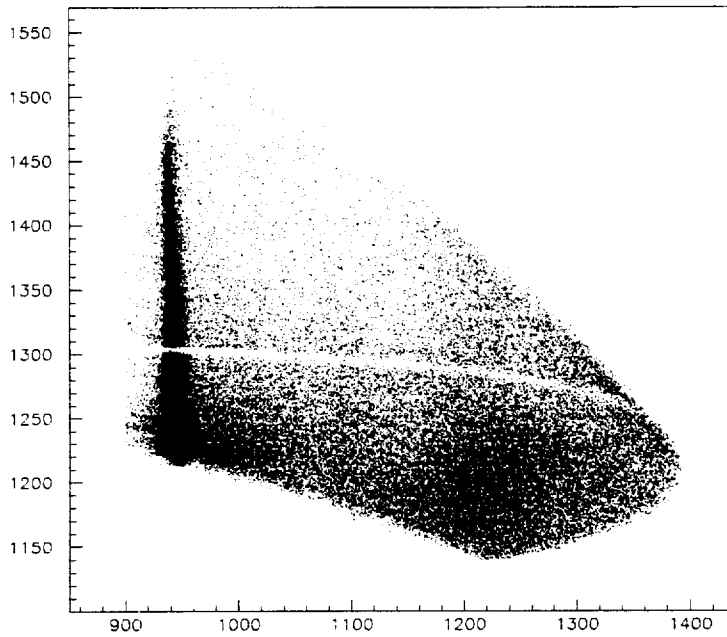


Fig.1. Invariant $p\pi^+$ mass against missing mass M_X events at 1805 MeV proton energy and 6.7° (mean angle value of both detected particles). The data clearly shows the production of Δ -n and two Δ events. The coordinates are expressed in MeV.

($\Delta\theta = \Delta\phi = \pm 50$ mrd) of the magnetic spectrometer. The cryogenic H_2 target was 393 mg/cm^2 thick. The detection consisted of several drift chambers followed by four planes of scintillating hodoscopes. The particle identification process, the determination of their trajectories and the correction of random coincidences were described elsewhere [22]. The proton beam polarizations were .78, .74 and .70 for the three increasing energies. Their values were reversed at each spill in order to avoid any bias due to a possible polarization drift.

In Fig.1 we show the $p\pi^+$ invariant mass versus the missing mass of events (before normalizations) obtained at 1805 MeV, 6.7° . On the left side the figure shows the neutron missing mass peak. These events are in coincidence with Δ superposed to p and π^+ in invariant mass. On the right side, the heavy dark region corresponds to two Δ production, Δ^0 and Δ^{++} in missing mass and invariant mass respectively, superposed to non resonant background.

The empty zone in Fig.1 corresponds to the same intersection of the two trajectories on the focal plane, where the first drift chamber was located. Such events were lost, as were lost all events when both trajectories intersected on all planes of the detection. A simulation code describing the detection has been written in order to correct the corresponding inefficiencies.

The limits of the plot are produced by the cuts on momenta : (600 and 1400 MeV/c), applied on both particles during the analysis, since they correspond to well defined acceptance of SPES 3. These limits move with incident energies

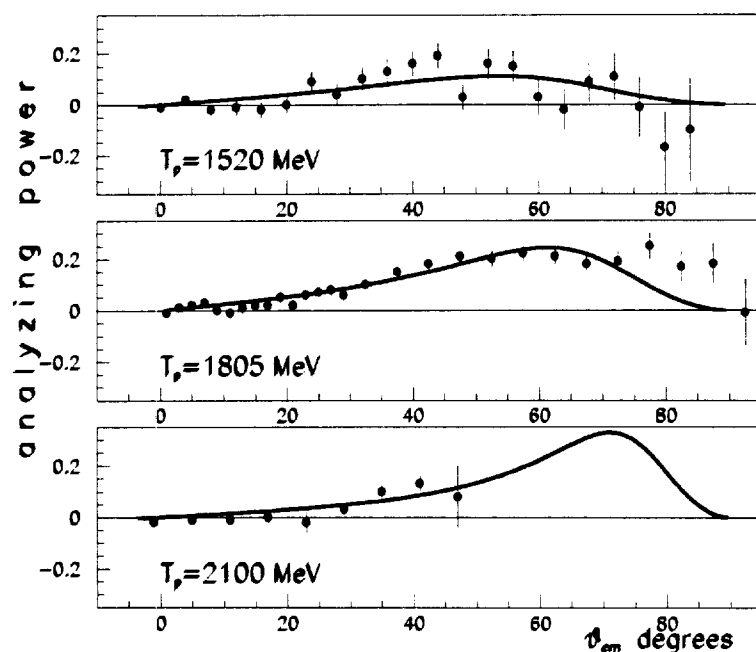


Fig.2. Analyzing powers at all three energies with and without Δ formation in the region of $\bar{p} p \rightarrow \Delta^{++} \Delta^0$ reaction. The curves are results of theoretical fits discussed in section 4.

and angles. The lowest energy : 1520 MeV, is suitable to the study of the $\bar{p} p \rightarrow \Delta n$ reaction, whereas 1805 MeV proton energy is appropriate to study the $\bar{p} p \rightarrow \Delta \Delta$ reaction. The highest energy : 2100 MeV is suitable to study higher missing and invariant masses.

Cuts were applied on different parts of the scatter plot displayed in Fig. 1 in order to select the three reactions considered. These cuts are given in the figure captions. The extraction of the peak analyzing powers is based on the assumption that the background analyzing power is a slow function of the missing and invariant masses, and therefore can be averaged between values on opposite sides.

3 Results

3.1 $\bar{p} p \rightarrow p \pi^+ X$ around $M_X = M_{p\pi} = M_\Delta$ and $\bar{p} p \rightarrow \Delta \Delta$ reactions

The last exclusive reaction has never been studied previously. The second figure shows the $\bar{p} p \rightarrow p \pi^+ X$ results for the three energies without separation of resonant and non resonant states, in the region of the $\bar{p} p \rightarrow \Delta^{++} \Delta^0$ reaction.

The events were selected using a circular cut of 80 MeV radius in the scatter plot $M_{p\pi^+}/M_X$ (Fig.1), whose central point was at $M_{p\pi^+}=M_X=M_\Delta$.

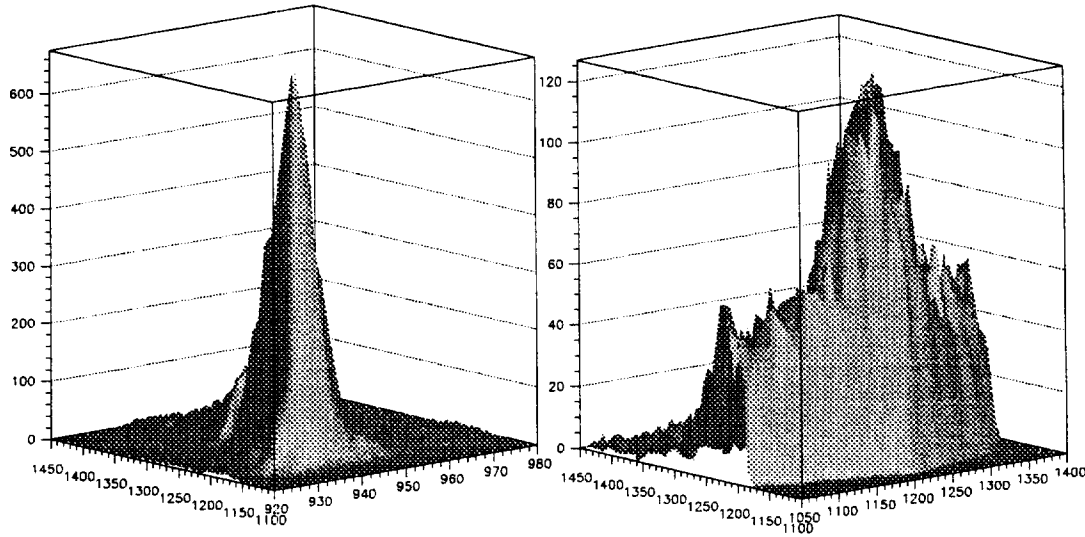


Fig.3 Three dimensional plot showing the invariant $M_{p\pi^+}$ mass versus the missing mass M_X data at 1520 MeV (left) and at 1805 MeV (right), both at 9° lab.

At 2100 MeV, no measurement exists for angles larger than 90° (lab.). The analyzing powers are close to zero until 20° , are positive for larger angles and cancel at 90° at the two lowest energies where data exists up to that angle. On Fig.3 (right), where a three dimensional plot shows the number of events against the invariant $M_{p\pi^+}$ mass and against the missing mass M_X , we clearly see a peak over a background. This makes it easy to separate the two reactions. At 1805 MeV, it was possible to study the evolution of the analyzing powers in the $\Delta^{++} \Delta^0$ region for peak plus background events. The cuts used to select the events have been defined by using different radii in the $M_{p\pi^+}/M_X$ scatter plot (Fig.1), at the central point of $M_{p\pi^+}=M_X=M_\Delta$. Figure 4 illustrates these results, successively for the central region (radius 20 MeV), and the crowns ($\delta(\Delta)$) between 20 and 40, 40 and 60 and finally between 60 and 80 MeV.

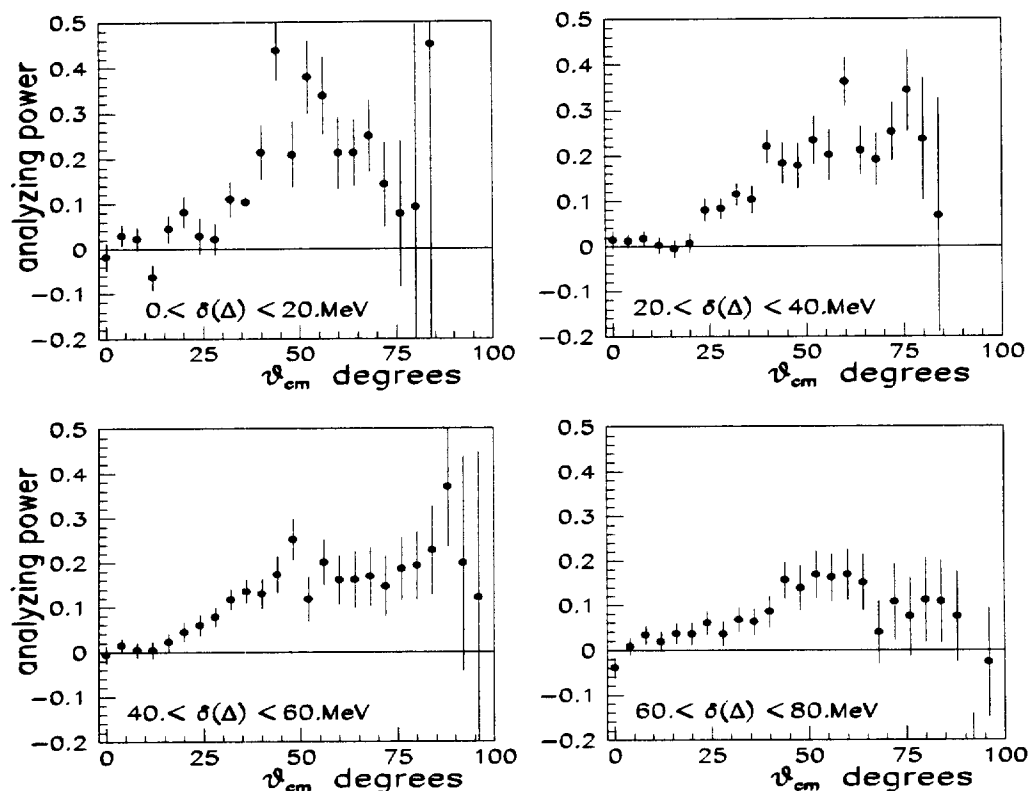


Fig.4. Analyzing powers at $T_p = 1805$ MeV for successive slices moving off from $M_{p\pi^+}=M_X=M_\Delta$ for the $\bar{p} p \rightarrow p \pi^+ X$ reaction.

In order to separate the peak from the background, we have defined the peak plus background region by a 80 MeV radius range in the $M_{p\pi^+}/M_X$ scatter plot (Fig.1), at the central point of $M_{p\pi^+}=M_X=M_\Delta$ for the peak, and a crown between 80 and 130 MeV radii for the background. The result is displayed in Fig. 5. The general shape of the distribution is close to that of the one observed before the background subtraction, indicating that the analyzing power without a two Δ formation is not very different from the one corresponding to a doubly resonant state.

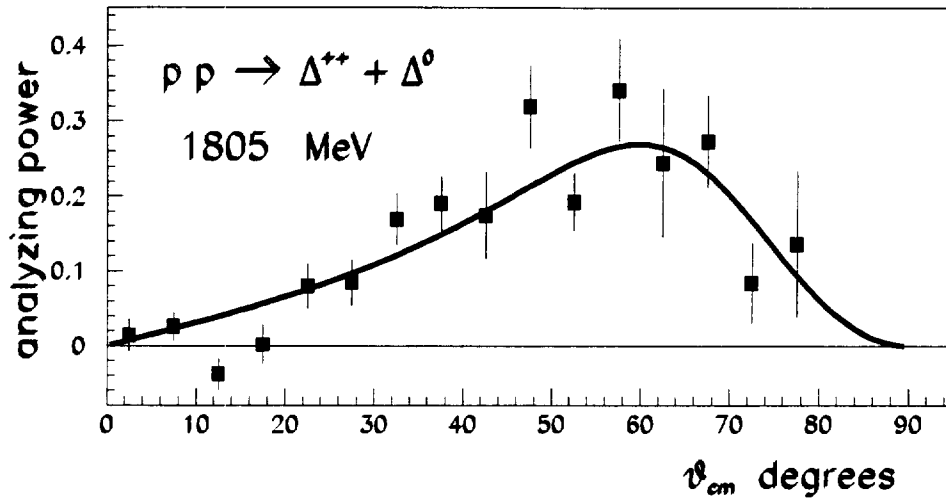


Fig.5. Analyzing powers with two Δ formation after background subtraction. The curve results from the theoretical fit discussed in section 4.

3.2 $\bar{p} p \rightarrow \Delta n$ and $\bar{p} p \rightarrow p \pi^+ n$ reactions

We see on Fig.3 (left), a cut for low values in invariant mass. The knowledge

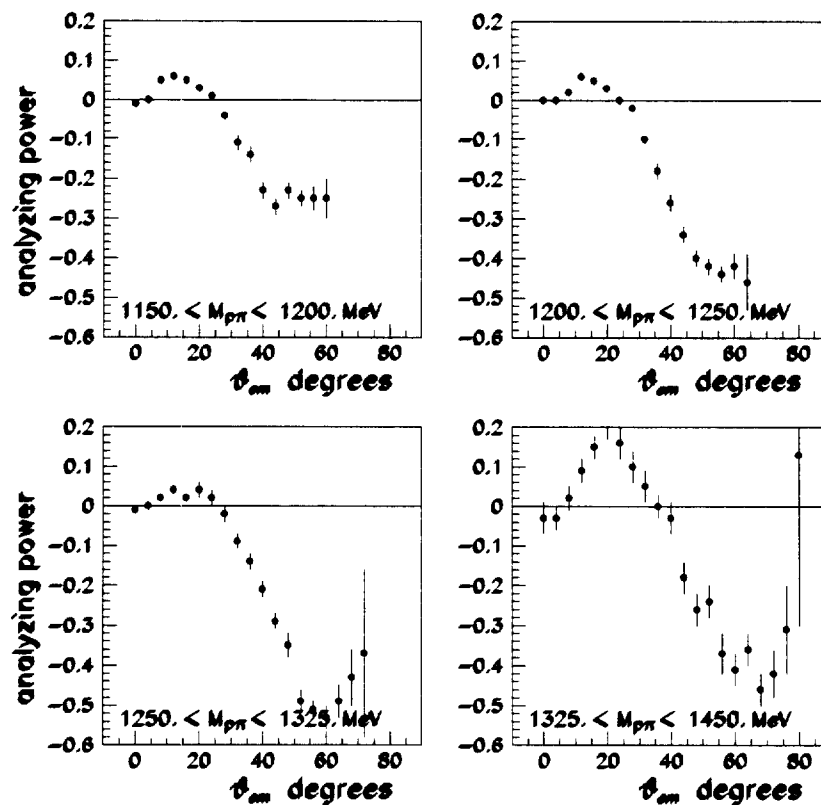


Fig.6. Analyzing powers at 1520 MeV for the $\bar{p} p \rightarrow p \pi^+ n$ reaction and different ranges of invariant $p\pi^+$ masses. The following cuts, $930 < M_X < 960$ MeV, were applied.

of the background shape for only large invariant masses, doesn't allow us to extract the Δn reaction from the $p n \pi^+$ reaction.

Figure 6 shows the analyzing powers at 1520 MeV for the following ranges of invariant $M_{p\pi^+}$ masses : $1150 < M_{p\pi^+} < 1200$ MeV, $1200 < M_{p\pi^+} < 1250$ MeV, $1250 < M_{p\pi^+} < 1325$ MeV and $1325 < M_{p\pi^+} < 1450$ MeV. The first ranges correspond to the $\bar{p} p \rightarrow \Delta n$ reaction since the Δ excitation predominates. The last range corresponds to the region where mixing of non resonant $p\pi^+$ events and tails from lower mass Δ (1232) and higher masses Δ (1600), (1620) and(1770) occurs.

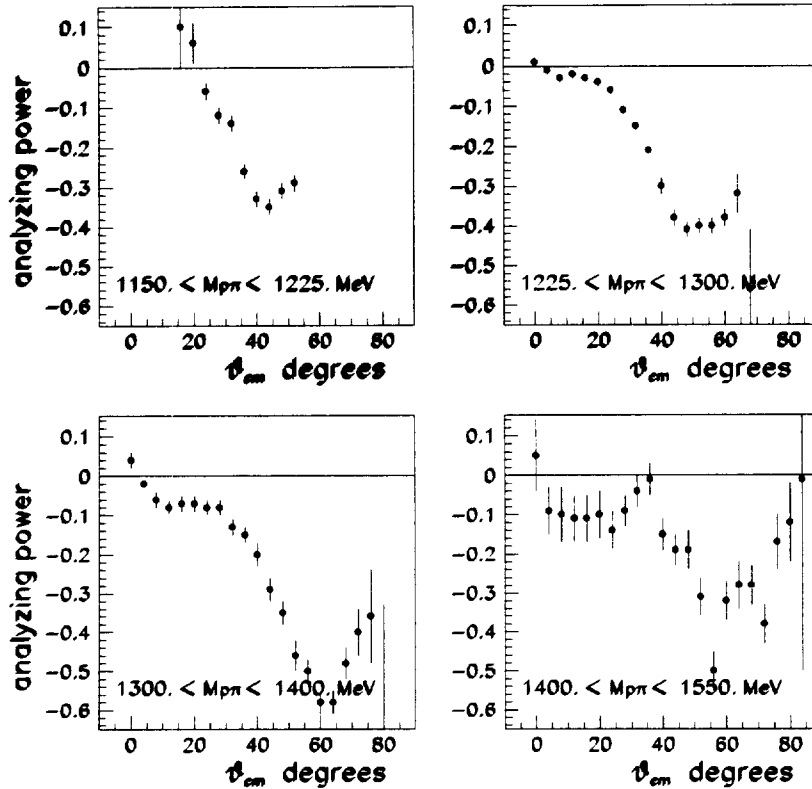


Fig.7. Analyzing powers at 1805 MeV for $\bar{p} p \rightarrow p \pi^+ n$ reaction and different ranges of invariant $p\pi^+$ masses. The following cuts have been applied $930 < M_X < 960$ MeV.

Figure 7 presents the same data for 1805 MeV incident protons. Here again, the first two selections $1150 < M_{p\pi^+} < 1225$ MeV and $1225 < M_{p\pi^+} < 1300$ MeV, correspond to the $\bar{p} p \rightarrow \Delta n$ reaction. The two last selections : $1300 < M_{p\pi^+} < 1400$ MeV and $1400 < M_{p\pi^+} < 1550$ MeV are for the $\bar{p} p \rightarrow p \pi^+ n$ reaction. Although the general shapes are not very different at both energies, a general decrease of the analyzing power is observed at 1805 MeV, with the beginning of the increase starting at an angle larger than 42° (not observed at 1520 MeV).

Unlike the previous reaction, some data was obtained for the $\bar{p} p \rightarrow \Delta n$

reaction at smaller energies than those studied in our experiment. Data was obtained at 0.4 and 0.45 GeV from TRIUMF [23], at 0.8 GeV in Los Alamos [24] [25], and at 1.18, 1.47, 1.71 and 1.98 GeV/c (0.57, 0.806, 1.012 and 1.253 GeV) in Argonne [26] .

4 Analysis

Different versions of the one-boson (π, ρ, ω and σ) exchange model are the basis for recent theoretical investigations of the $N N \rightarrow \Delta \Delta$ and the $N N \rightarrow \Delta n$ reactions at low and intermediate energies ($T_p \leq 1.25 \text{ GeV}$). The results obtained in LAMPF [27] were analyzed in an attempt to compare them with the predictions of the relativistic three-body model [28].

Using different meson-nucleon coupling constants and effective form factors to simulate rescattering effects, the calculated total and differential cross-sections [29] were in agreement with the data. However the one-boson exchange model produces real amplitudes and therefore no T-odd polarization observables. The iterated pion-exchange model [28] takes care of two and three body unitarity and produces non-zero T-odd polarization observables. However, for $T_p = 0.8, 1.0$ and 1.2 GeV the calculations performed within that model, found a positive \mathcal{A}_y , which is in contradiction with the experimental data [26]. The results from Argonne were analyzed within the coupled $\pi^+ NN$ - NN model [30]. These calculations gave rise to satisfactory cross-sections, but also gave rise to a poor agreement for the asymmetry since at 806 MeV, even the sign is inverted. It has been stressed [31] that the $N N \rightarrow \Delta n$ reaction is less peripheral than often believed. In [31] the short range contributions were described by a ρ exchange using three parameter fits. However the resulting coupling constants moved with energy and a phase has been arbitrarily introduced in the ρ exchange matrix element.

We have suggested in the present work another approach, consistent with the central properties of these reactions. It is based on s-channel contribution only with a relatively small ($\ell \leq 2$) orbital momenta of the produced particles, since we are not far from threshold. The $J^P = 2^+$ intermediate state is important since close to $N\Delta$ threshold, the $N N$ interaction is strongly inelastic and exhibits a resonant-like behaviour in 1D_2 ($N N$) and 3F_3 ($N N$) waves. In order to get a non zero analyzing power, we need an interference in the s-channel of the 2^+ partial singlet amplitude with triplet amplitudes, which corresponds to pp collisions with odd orbital momenta value, i.e. with negative P parity . We add therefore the $J^P = 1^-$ wave to the 2^+ wave. In a simplified version of such an approach, it is possible to fit the θ dependence of \mathcal{A}_y for $\bar{p} p \rightarrow \Delta^{++} \Delta^0$ reaction with 2 parameters only. These parameters describe the relative role of the two partial amplitudes and their relative phase. However, due to the large number of possible partial amplitudes in $J^P = 1^-$ and 2^+ intermediate

states for the $\bar{p} p \rightarrow \Delta^{++} n$ reaction, we use a general parameterization of \mathcal{A}_y with 4 parameters, which is correct for any combination of the allowed partial transitions.

4.1 Discussion for $\bar{p} p \rightarrow \Delta^{++} \Delta^0$ reaction

The general formula (see appendix for its derivation) is:

$$\mathcal{A}_y = -1.5 R \sin\delta \times \frac{\sin\theta \cos^2\theta}{1 + 5/8 R^2 \cos^4\theta} \quad (1)$$

where $R = |g_2|/|g_1|$ and δ is the relative phase between both amplitudes. The fits obtained using this relation are plotted in Fig.2. Both parameters R and δ have been fitted at 1.52 and 1.805 GeV. At 2.1 GeV there are not enough results to allow us to determine both parameters. Therefore, at this energy the phase was fixed by an extrapolation from the values obtained at the two lowest energies. Then R was fitted. Since the data plotted in Fig.2, at all three energies correspond to analyzing powers with and without Δ formation, the same fit was done at 1.805 GeV on data obtained after background subtraction. The resulting curve is plotted in Fig.5. The corresponding values of χ^2 are 1.4 and 1.8 for 1520 and 1805 MeV respectively, in the case of peak + background

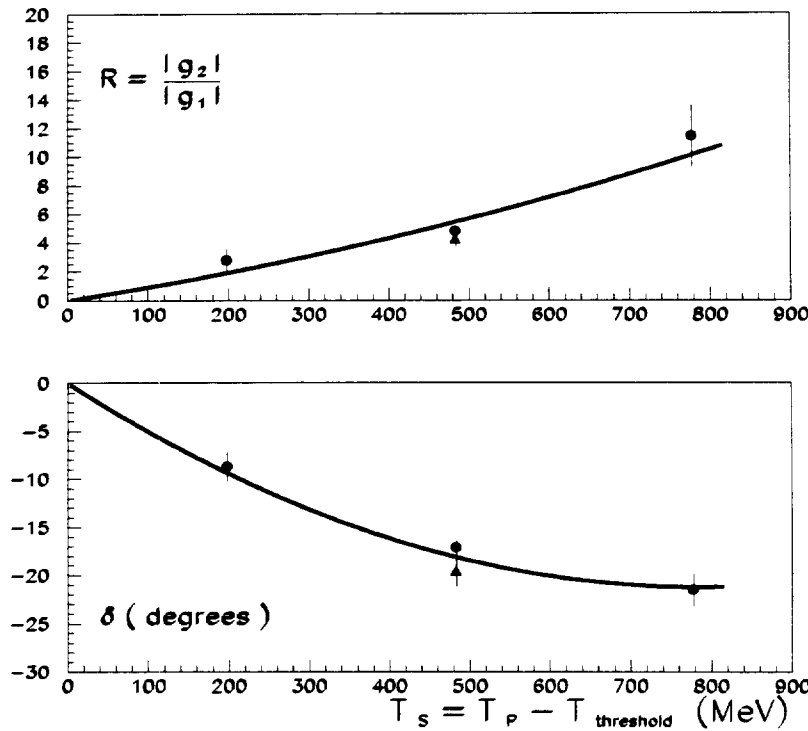


Fig.8. Values of R and δ parameters obtained from the analyzing power of $\bar{p} p \rightarrow \Delta^{++} \Delta^0$ reaction using formula [1].

fits, and 2.2 at 1805 MeV for the fit of the data after background subtraction. Fig.8 shows the values obtained for both parameters with (black circles) and without (black triangles) background, displayed against the energy shift from the threshold. We observe an agreement between parameters obtained with and without background. This demonstrates quantitatively that the analyzing power of the $\bar{p} p \rightarrow \Delta^{++} \Delta^0$ reaction is very close to that of the background in the same mass region. Both parameters display a continuous behaviour. The extrapolation of the phase shift δ is compatible with zero at the threshold. The variation of R and δ allows us to find the relative positions of both resonances. The 2^+ resonance is at a smaller mass than the 1^- but close to 2.73 GeV (corresponding to $T_p = 2100$ MeV.)

4.2 Discussion for $\bar{p} p \rightarrow \Delta^{++} n$ reaction

The general formula (see appendix for its derivation) is:

$$A_y = \sin\theta \times \frac{a + b \cos^2\theta}{1 + c \cos^2\theta + d \sin^2\theta \cos^2\theta} \quad (2)$$

where a,b,c and d are real parameters which depend on the energy of colliding particles and are determined by the definite combinations of partial amplitudes. Figure 9 displays the fits obtained at 1520 and 1805 MeV using the previous relation. Although there are four adjusted parameters, the agree-

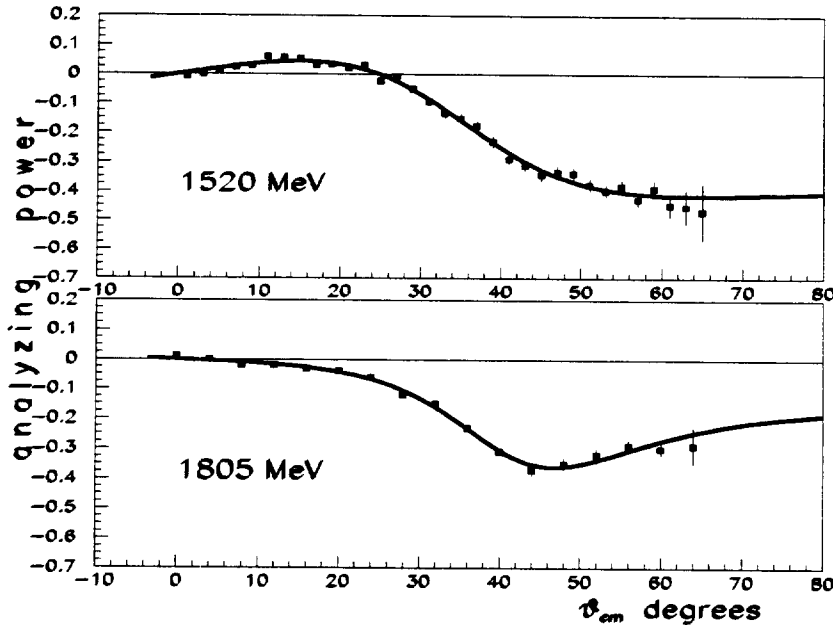


Fig.9 Analyzing powers in the region of $\bar{p} p \rightarrow \Delta^{++} n$ reaction ($1170 \leq M_{p\pi^+} \leq 1270$ MeV). The curves were obtained using equation (2). The related parameters are presented in table 1.

	a	b	c	d	χ^2
1520 MeV	$-.40 \pm .02$	$.49 \pm .02$	$-.65 \pm .02$	$-1.33 \pm .09$	1.53
1805 MeV	$-.18 \pm .02$	$.14 \pm .03$	$-.35 \pm .10$	$-2.44 \pm .22$	0.89

Table 1. Fitted values of the coefficients of equation (2) corresponding to $\bar{p} p \rightarrow \Delta^{++} n$ reaction.

ment here is significant, which indicates that the processes considered may very well be the main ones.

4.3 General discussion

The suggested description for the angular dependence of the analyzing power for reactions $\bar{p} p \rightarrow \Delta^{++} n$ and $\bar{p} p \rightarrow \Delta^{++} \Delta^0$ can be considered to be “orthogonal” to OBE models. Such OBE models (with different t channel exchanges) are often used to describe reactions with meson or Δ production : $p p \rightarrow \pi^0(\eta)pp$, $p p \rightarrow \Delta^{++} n$, $p p \rightarrow \Delta^{++} \Delta^0$ as well as others reactions.

Is it possible to add these s and t -channels contributions in order to obtain a complete description of the previous reactions ? Such a procedure was used for pion photo- and electro-production, $\gamma N \rightarrow N \pi$ and $e^- N \rightarrow e^- N \pi$, in the resonance energy region.

The main problem here is to avoid double counting. Indeed all OBE calculations for reactions involving hadrons must be improved by the addition of rescattering graphs which correspond to strong interactions in the initial and the final states (unitarization procedure). When such interactions are strong (for states of NN system with definite values of J^P), the OBE diagrams can be transformed to s -channel diagrams. This is illustrated in Fig.10. Therefore a simple addition of t and s -channel contributions will result in double counting. It will also violate unitarity.

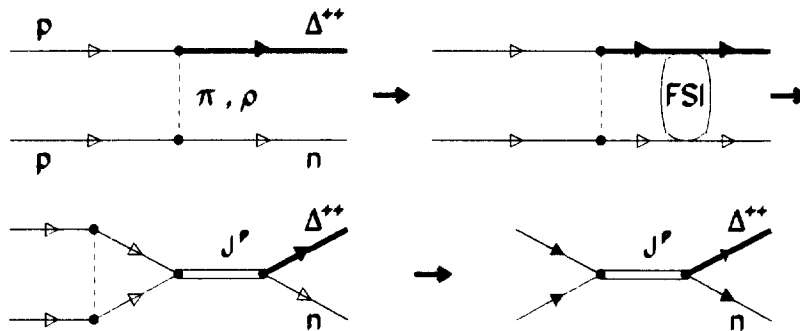


Fig.10. Feynman diagrams showing the transformation from t -channel with strong final state interactions to s -channel graphs.

Note also, that duality arguments prevent such simple addition, since duality means that the sum of all possible t-channel exchanges is equivalent to the sum of the important s-channel contributions.

5 Conclusion

In conclusion, analyzing powers for inelastic \bar{p} p scattering were measured at the following proton energies : 1520, 1805 and 2100 MeV. This new data concerns the following three reactions : \bar{p} p \Rightarrow Δ^{++} Δ^0 , \bar{p} p \Rightarrow Δ^{++} n and \bar{p} p \Rightarrow p π^+ X. It should be used, combined with previous existing data from elastic and inelastic N-N scattering in order to constrain the coupled-channel analysis and allow an unified theoretical description of the N-N interaction.

The angular behaviour of the analyzing power in \bar{p} p \rightarrow Δ^{++} n and \bar{p} p \rightarrow $\Delta^{++}\Delta^0$ supports definitively the importance of central collisions in the energy region considered in this work. The s-channel description of these reactions (in terms of $J^P = 1^-$ and 2^+ intermediate states) can be considered as being a simple and successful attempt to describe the data. Such description must also be important for other reactions as the elastic p p scattering. Indeed, such exotic states (possible broad dibaryon resonances) have been observed [32] in the polarization phenomena in p p scattering, namely in the singlet state (mass ≈ 2.77 GeV, $T_p = 2.1$ GeV). Following [33] this state is the lowest exotic 6 q configuration with I=1. The agreement observed indicates that the processes considered might be the main processes for these reactions close to threshold.

Acknowledgments

We thank J. Van de Wiele for helpful discussions concerning the theoretical part. One of the authors (M.P.R.) would like to express his deep gratitude for the hospitality of L.N.S. and I.P.N. Orsay , and thanks F.Lehar for interesting discussions on dibaryon problems. We are grateful to Natalie Lutz for help in writing our manuscript in English.

References

- [1] C.Lechanoine-Leluc and F.Lehar Rev.Mod.Phys. **65** (1993) 47.
- [2] W.K.Pitts *et al.* Phys.Rev. **C45** (1992) R1; *ibid* Phys.Rev. **C45** (1992) 455.

- [3] Y.Kobayashi *et al.* Nucl.Phys **A569** (1994) 791.
 - [4] G.Glass *et al.* Phys.Rev. **C45** (1992) 35.
 - [5] J.Nagata, H.Yoshino and M.Matsuda Prog.Theor.Phys. **93** (1995) 559.
 - [6] Y.Terrien *et al.* Phys.Rev.Lett. **59** (1987) 1534. J.Ball *et al.* Nucl.Phys **A559** (1993) 477; *ibid* Nucl.Phys **A559** 489 (1993); *ibid.* Nucl.Phys **A559** (1993) 511.
 - [7] K.H.McNaughton *et al.* Phys.Rev. **C46** (1992) 47; W.B.Tippens *et al.* Phys.Rev. **C36** (1987) 1413.
 - [8] H.Garcilazo and T.Mizutani π NN Systems, World Publishing Co., (1990) 1.
 - [9] T.Tsuboyama, N.Katayama, F.Sai and S.S.Yamamoto Nucl.Phys. **A486** (1988) 669.
 - [10] R.L.Shypit *et al.* Phys.Rev. **C40** (1989) 2203.
 - [11] R.L.Shypit *et al.* Nucl.Phys **A477** (1988) 541; D.V.Bugg *et al.* Nucl.Phys **A477** (1988) 546.
 - [12] D.A.Barlow *et al.* Phys.Rev. **C37** (1988) 1977.
 - [13] N.Tanaka *et al.* Phys.Rev. **C37** (1988) 2071.
 - [14] Chang Heon Oh *et al.* Phys.Rev. **C56** (1997) 635.
 - [15] H.Garcilazo and T.Mizutani Few-Body Systems **5** (1988) 127.
 - [16] T.Ueda Nucl.Phys. **A573** (1994) 511.
G.M.Shklyarevsky J.Phys.G. Nucl.Part.Phys. **17** (1991) 85.
 - [17] B.E.Bonner *et al.* Phys.Rev. **D27** (1983) 497.
 - [18] T.Mizutani, C.Fayard, G.H.Lamot and B.Saghai Phys. Rev. **C40** (1989) 2763.
 - [19] C.Fayard, G.H.Lamot, T.Mizutani and B.Saghai Phys.Rev. **C46** (1992) 118.
 - [20] J.P.Auger, C.Lazard Phys.Rev. **C52** (1995) 513.
 - [21] M.P.Comets *et al.* IPNO DRE 88-41, Internal Report.
 - [22] B.Tatischeff, J.Yonnet, N.Willis *et al.* Phys.Rev.Lett. **79** (1997) 601.
 - [23] W.R.Falk *et al.* Phys.Rev. **C32** (1985) 1972.
 - [24] A.D.Hancock *et al.* Phys.Rev. **C27** (1983) 2742.
 - [25] C.L.Hollas *et al.* Phys.Rev.Lett. **55** (1985) 29.
 - [26] A.B.Wicklund *et al.* Phys.Rev. **D34** (1986) 19; **D35** (1987) 2670.
 - [27] J.Dubach *et al.* Phys.Rev. **C34** (1986) 944.
 - [28] W.M.Kloet and R.R.Silbar Nucl.Phys. **A338** (1980) 281. Nucl.Phys. **A364** (1981) 346.
-

- [29] S.Huber, J.Aichelin Nucl.Phys. **A573** (1994) 587.
 [30] T.Mizutani, C.Fayard, G.H.Lamot and B.Saghai Phys.Rev. **C47** (1993) 56.
 [31] J.P.Auger, C.Lazard and R.J.Lombard Phys.Rev. **D39** (1989) 763.
 [32] C.E.Allgower *et al.* Eur.Phys.J., **C1** (1998) 131.
 [33] E.L.Lomon Colloque de Physique (France), **51** (1990) C6-363.

6 Appendix

6.1 Reaction $\vec{p} p \rightarrow \Delta^{++} \Delta^0$

We shall consider for this process only two partial transitions, corresponding to $J^P = 1^-$ and 2^+ .

Taking into account a generalized Pauli principle (isotopic invariance) for $\Delta^{++} + \Delta^0$ - system and the usual Pauli principle for colliding protons, the following transitions are allowed for the $J^P = 1^-$:

$$\begin{aligned} S_i = 1, l_i = 1 \rightarrow J^P = 1^- \rightarrow S_f = 1, l_f = 1 \\ \rightarrow S_f = 3, l_f = 3 \end{aligned}$$

So, the matrix element for P - wave production can be written as follows :

$$\mathcal{M}(J^P = 1^-) = g_1(s) [\widetilde{\chi}_2 \sigma_2 (\vec{\sigma} \times \vec{k})_a \chi_1] [\varphi_{2a}^+ \sigma_2 \vec{\varphi}_1^+ \cdot \vec{q} - \vec{\varphi}_2^+ \cdot \vec{q} \sigma_2 \widetilde{\varphi}_{1a}^+] \quad , \quad (3)$$

where the following notations have been used:

- χ_1 and χ_2 are the 2-components spinors of the colliding protons
- \vec{k} and \vec{q} are the 3-momentum unit vectors of the colliding and the final particles (in CMS of the reaction)
- $\vec{\varphi}_1$ and $\vec{\varphi}_2$ are the 2 - component spinors for produced Δ^{++} and Δ^0 , respectively
- $g_1(s)$ is the P-wave partial amplitude.

For $J^P = 2^+$ the conservation of total angular momentum and P - parity allows the following transitions :

$$\begin{aligned} S_i = 0, l_i = 2 \rightarrow S_f = 0, l_f = 2 \\ \rightarrow S_f = 2, l_f = 0 \end{aligned}$$

$$\begin{aligned} &\rightarrow S_f = 2, \ell_f = 2 \\ &\rightarrow S_f = 2, \ell_f = 4 \end{aligned}$$

The matrix element for the singlet $\Delta\Delta$ - production can be written as follows :

$$\mathcal{M}(J^P = 2^+) = g_2(s) [\widetilde{\chi}_2 \sigma_2 \chi_1] [\varphi_{2a}^+ \sigma_2 \widetilde{\varphi}_{1a}^+] [\mathcal{L}_{ab}(k)][\mathcal{L}_{ab}(q)] . \quad (4)$$

In the previous relation, in order to describe the orbital momenta $\ell_i = 2$ and $\ell_f = 2$, the following notations were used respectively:

$$\mathcal{L}_{ab}(k) = k_a k_b - \frac{1}{3} \delta_{ab} , \quad \mathcal{L}_{ab}(q) = q_a q_b - \frac{1}{3} \delta_{ab} .$$

and $g_2(s)$ is the D-wave partial amplitude.

If ones sums up the polarizations of both Δ 's and averages the polarization states of target, we end up with the following formula (1).

6.2 Reaction $\vec{p} p \rightarrow \Delta^{++} n$

Taking into account firstly the Pauli principle for colliding identical particles, and secondly the conservation of total angular momentum and P-parity, one can find that the following partial transition are allowed for the $J^P = 1^-$ (of the s-channel of reaction $\vec{p} p \rightarrow \Delta^{++} n$) :

$$\begin{aligned} S_i = 1, \ell_i = 1 &\rightarrow S_f = 1, \ell_f = 1 \\ &\rightarrow S_f = 2, \ell_f = 1 \\ &\rightarrow S_f = 2, \ell_f = 3 \end{aligned} \quad (5)$$

where $S_i(S_f)$ is the total spin of the initial p p (final ΔN) - system, and where $\ell_i(\ell_f)$ is the orbital angular momentum of the colliding (final) particles in the CMS of the reaction being studied.

The most compact parameterization of the spin structure of corresponding contributions to the matrix elements can be done using 2-components formalism to describe nucleons and Δ -isobar (with spin 3/2).

6.2.1 Transition $S_i = 1, \ell_i = 1 \rightarrow S_f = 1, \ell_f = 1$

We can write :

$$\mathcal{M} = [\widetilde{\chi}_2 \sigma_2 (\vec{\sigma} \times \vec{k})_a \chi_1] [\vec{\varphi}^+ \times \vec{q}]_a \sigma_2 \widetilde{\chi}_1^+ g_{11}^{(P)} \quad (6)$$

where the following notations are, in addition to the previous ones :

- χ is the 2-component spinor of the final nucleon,
- $\vec{\varphi}$ is the specific 2-component spinor (each component of which is a vector) for describing the Δ -isobar,
- $g_{11}^{(P)}$ is the partial amplitude of the considered transition.

Spinor $\vec{\varphi}$ must satisfy the condition $\vec{\sigma} \cdot \vec{\varphi} = 0$, to describe only spin 3/2. The sum over polarization states of Δ - resonance is obtained using the formula

$$\overline{\varphi_a \varphi_b^\dagger} = \frac{4}{3}(\delta_{ab} - \frac{i}{2}\epsilon_{abc}\sigma_c).$$

The dependence on \vec{P} polarization of the proton beam can be taken into account by using the formula :

$$\overline{\varphi_1 \varphi_1^\dagger} = \frac{1}{2}(1 + \vec{\sigma} \cdot \vec{P})$$

6.2.2 Transition : $S_i = 1, \ell_i = 1 \rightarrow S_f = 2, \ell_f = 1$

The matrix element can be written as follows :

$$\mathcal{M} = i g_{12}^{(P)} [\chi_2^\dagger \sigma_2 (\vec{\sigma} \times \vec{k})_a \chi_1] [\varphi_a^\dagger \vec{\sigma} \cdot \vec{q} \vec{\sigma}_2 \widetilde{\chi}^+ + \vec{\varphi}^\dagger \cdot \vec{q} \sigma_a \sigma_2 \widetilde{\chi}^+] \quad (7)$$

where $g_{12}^{(P)}$ is the corresponding partial amplitude. It is important to note, that all partial amplitudes are complex functions of the single variable s . Due to the large centrifugal barrier for Δ - N production with $\ell_f = 3$, we will neglect this contribution. Excitation of $J^P = 2^+$ intermediate state in s-channel of reaction $\vec{p} p \rightarrow \Delta^{++} N$ is possible in the following set of partial transitions :

$$\begin{aligned} S_i = 0, \ell_i = 2 &\rightarrow S_f = 2, \ell_f = 0 \\ &\rightarrow S_f = 1, \ell_f = 2 \\ &\rightarrow S_f = 2, \ell_f = 2 \\ &\rightarrow S_f = 2, \ell_f = 4 \end{aligned} \quad (8)$$

In our 2 - component formalism the spin structure of corresponding transitions can be written in the following way :

$$\begin{aligned} \mathcal{M} = & g_{20}^{(D)} [\tilde{\chi} \sigma_2 \chi_1] [\varphi_a^\dagger \sigma_b \sigma_2 \widetilde{\chi}^+] \mathcal{L}_{ab}(k) + \\ & g_{22}^{(D)} [\tilde{\chi}_2 \sigma_2 \chi_1] [\varphi_a^\dagger \sigma_b \sigma_2 \widetilde{\chi}^+] [\mathcal{L}_{ac}(k)] [\mathcal{L}_{bc}(q)] + \\ & g_{12}^{(D)} [\tilde{\chi}_2 \sigma_2 \chi_1] [(\vec{\varphi}^\dagger \times \vec{q})_a \sigma_2 \widetilde{\chi}^+] [\mathcal{L}_{ab}(k) q_b] \quad , \end{aligned} \quad (9)$$

The cross-section dependence of the $\vec{p} p \rightarrow \Delta^{++} n$ reaction on the beam polarization \vec{P} is:

$$\frac{d\sigma}{d\Omega}(\vec{p} p \rightarrow \Delta^{++} N) = (1 + \mathcal{A}_y \vec{n} \cdot \vec{P}) \left(\frac{d\sigma}{d\Omega}\right)_0, \quad (10)$$

where $\vec{n} = \vec{k} \times \vec{q} / |\vec{k} \times \vec{q}|$ and $(\frac{d\sigma}{d\Omega})_0$ is the differential cross-section for unpolarized particles.

Since the two particles p and π^+ were detected in the same solid angle ($\pm 50 mrd$), the assumption that the Δ^{++} decayed in a collinear kinematics, is a completely justified assumption. Therefore, the experiment selects only Δ^{++} produced with helicity $\lambda_\Delta = \pm 1/2$, which means that the Δ^{++} are polarized. Then the angular dependences of $(\frac{d\sigma}{d\Omega})_0$ and \mathcal{A}_y are different from their expressions for unpolarized particles.

If we take into account all transitions through $J^P = 1^-$ and 2^+ intermediate states in addition to the production of polarized Δ^{++} ($\lambda_\Delta = \pm 1/2$), the general formula (2) can be obtained.